Magalhães, Augusto; Emzir, Muhammad; Corona, Francesco

Sparse Spectral Methods for Approximating PDE Solutions in Particle Flow

Published in:
Proceedings of the 2025 SIAM Conference on Control and Its Applications

DOI:
10.1137/1.9781611978742.8

Published: 01/01/2025

Document Version
Peer-reviewed accepted author manuscript, also known as Final accepted manuscript or Post-print

Sparse Spectral Methods for Approximating PDE Solutions in Particle Flow

Augusto Magalhães* Muhammad Emzir† Francesco Corona*

Abstract

In sequential Monte Carlo, a method for performing the Bayesian computation *prior* × *likelihood* is to derive the law of motion of a particle ensemble: a particle flow. This enables sampling from complex distributions while avoiding issues such as particle degeneracy and the need for resampling. However, some particle-flow implementations require solving a partial differential equation (PDE) whose coefficients depend on the density of particles. The solution to this PDE must typically be approximated as analytical solutions are limited to specific cases. Traditionally, spectral methods for approximating the solution are based on the tensor product formulation in which the solution is represented as a weighted sum of products of univariate basis functions. Using N_B bases per coordinate of the N_X-dimensional domain leads to $(N_B)^{N_X}$ unknowns. Thus, even for problems of moderate dimensionality, current computational resources are insufficient to support the full tensor-product grid necessary for an accurate approximation. In this work, we propose an approximation based on a sparse grid/hyperbolic cross technique to solve the PDE in more general settings. The solution is approximated with multivariate polynomials bases whose span is dense in the space of solutions under mild assumptions on the underlying distribution. We show the accuracy of our technique for sampling from Gaussian and non-Gaussian distributions.

1 Introduction.

Let $\mathbb{S}_X$ be a complete separable metric space, e.g. $\mathbb{S}_X \subseteq \mathbb{R}^{N_X}$, $N_X \geq 1$. In this work, we construct a sparse spectral method for solving the elliptic equation

$$
\begin{aligned}
&-\nabla \cdot (\alpha(x) \cdot \beta(x) \nabla \phi(x)) = m(x)\,\alpha(x), \\
&\int_S m(x)\,\alpha(x)\,dx = 0,\ x \in S,\ S \subseteq \mathbb{S}_X,
\end{aligned}
\tag{1.1}
$$

where ∇ and $\nabla \cdot (\cdot)$ denote, respectively, the gradient and divergence operators, $\phi : S \to \mathbb{R}$ is the function of interest, and the coefficients are mappings of the form $\alpha : S \to \mathbb{R}_+$, $\beta : S \to \mathbb{R}^{N_X} \times \mathbb{R}^{N_X}$, and $m : S \to \mathbb{R}$. Notably, the condition $\int_S m(x)\,\alpha(x)\,dx = 0$ is equivalent to a Neumann boundary condition on the boundary ∂S of a set S within which x is constrained.

In general, (1.1) describes the potential associated with the transport of particles *i*) modulated by interactions captured by β; *ii*) following a gradient-type flow, i.e. $\nabla\phi$; and *iii*) driven by a source term m which represents local imbalances in the generation or depletion of particles at different points in the domain. In the case of a constant coefficient α, say $\alpha(x) \equiv 1$, this elliptic partial differential equation (PDE) is reduced to the Poisson equation, describing the potential associated with the transport of particles uniformly distributed over S. For a varying coefficient α, PDE (1.1) generalises the flow to account for particles distributed with spatial weighting. Herein, we refer to the general form of PDE (1.1) as the weighted Poisson equation, similarly to [1].

Except for specific cases, the weighted Poisson equation has no available analytical solution, and ϕ must be numerically approximated. We aim to approximate ϕ *i*) without restrictive assumptions on α other than $\alpha(x) \propto \exp(-V(x))$ with mild growth conditions on V, and *ii*) under the context of particle-based approximations, that is, ϕ is to be evaluated on Monte Carlo particles. Within this context, several methods have been proposed in the literature. These primarily include diffusion map-based approaches using a semigroup formulation [1], as well as spectral methods based on a weak formulation [2, 3]. A recent study comparing these approaches can be found in [4].

Traditional spectral methods for solving PDEs rely on a tensor product [5]. In this case, the challenge is evident in the error decay rate in terms of the total number of unknowns. A typical error estimate for an approximation $\widehat{\phi}$ is

$$
\|\widehat{\phi} - \phi\|_{\mathcal{H}^1_\alpha(S)} \leq c(N_X)\, N_B^{-r/N_X}\, \|\phi\|_{\mathcal{H}^{1+r}_\alpha(S)},
\tag{1.2}
$$

where the norms are in Hilbert spaces weighted by the coefficient α, $N_B \in \mathbb{N}$ is a discretisation parameter, $r \in \mathbb{N}$ is the isotropic smoothness of ϕ, and c is a constant which may depend on N_X but not on N_B [6]. Notably, (1.2) shows that the error estimate deteriorates exponentially with the dimension N_X, an issue known as the "curse of dimensionality".

In this study, we work with sparse grid discretisation methods for PDEs to circumvent the exponential deteri-

*Department of Chemical and Metallurgical Engineering, Aalto University, Espoo, FI.

†Control and Instrumentation Engineering Department, King Fahd University of Petroleum and Minerals, Dhahran, SA.

oration with N_X. In particular, we focus on the methods known as hyperbolic cross (HC) approximations. In such approximations, the convergence rate is either slowly deteriorated by a term $N_B^{-r}(\log N_B)^{(N_X-1)(r+1)}$, or, in a better scenario, the dimension impacts the convergence rate only through the constant c. However, these convergence results are based on HC approximations applied to generalised Hermite polynomials as the basis for ϕ [7], and assume that ϕ belongs to $\mathcal{L}^2(S)$, the space of square-integrable functions on S. This is not a desirable result for our applications. First, to the best of our knowledge, there exists no systematic way of choosing a basis for ϕ, which has been one of the main challenges of the weak formulation. Secondly, ϕ solving PDE (1.1) is often only in $\mathcal{L}^2_\alpha(S)$, i.e. ϕ is a square-integrable function on S with respect to varying coefficients α. For instance, in the case of $S = \mathbb{R}$, $m(x) = x$, and $\alpha(x) \propto \exp(-x^2)$, often discussed in the state estimation literature [4], the solution is $\phi(x) \propto x$, hence $\phi \notin \mathcal{L}^2(\mathbb{R})$. Thus, decaying polynomials studied in [7] do not approximate ϕ well.

The first contribution of this paper is the proposed choice of basis whose span is dense in $\mathcal{L}^2_\alpha(S)$, guaranteeing that the bases are sufficiently rich to approximate any solution ϕ. The second contribution is the novel application of HC approximations to the case of a varying α. Our intent is to combine these two contributions to achieve more efficient numerical solutions to PDE (1.1) beyond the well-documented univariate case.

The rest of this paper is organised as follows: §2 provides a compact overview of the problem. In particular, §2.1 describes the weak formulation of the weighted Poisson equation, and §2.2 concerns the representation of solutions by basis functions. §3 introduces our choice of basis and the use of smoothing estimates as a tool to improve approximations. §4 describes the main ingredients of HC approximations. §5 concerns the solution to the weighted Poisson equation when the coefficient α is the density of a probability distribution. More specifically, we present numerical results for the case of Bayesian sampling. §6 concludes the paper with some remarks.

2 Preliminaries.

We introduce the notation in Table 1 for clarity.

Table 1: Notation summary.

Set/Space	Elements
$\mathbb{N}_0$	$\mathbb{N} \cup \{0\}$ (natural numbers including zero)
D^r	r-th order differentiation, $r \in \mathbb{N}_0$
$C^r(S)$	r-times continuously differentiable functions, $r \in \mathbb{N}_0$
$\mathcal{L}^2(S)$	Square integrable functions on S
$\mathcal{L}^2_\alpha(S)$	Square integrable functions on S w.r.t. α
$\mathcal{L}^\infty(S)$	Functions bounded almost everywhere on S
$\mathcal{H}^r(S)$	Hilbert space functions whose first r derivatives are in $\mathcal{L}^2(S)$
$\mathcal{H}^r_\alpha(S)$	α-weighted Hilbert space functions whose first r derivatives are in $\mathcal{L}^2_\alpha(S)$
$\mathcal{H}^r_{\alpha,0}(S)$	Functions v in $\mathcal{H}^r_\alpha(S)$ with the additional condition $\int_S v(x)\,\alpha(x)\,dx = 0$

2.1 The weak formulation of the weighted Poisson equation.

The equality in PDE (1.1) is valid if ϕ is twice differentiable. To relax this condition, we seek a solution to the weak form of this PDE via an arbitrary test function $\eta \in \mathcal{H}^1_\alpha(S)$. By multiplying PDE (1.1) by η on both sides, and integrating the resulting equation over S, we obtain

$$-\int_S \nabla \cdot (\alpha(x) \cdot \beta(x) \nabla\phi(x))\,\eta(x)\,dx = \int_S m(x)\,\alpha(x)\,\eta(x)\,dx.$$

By integration by parts,

$$\int_S \alpha(x) \cdot \beta(x) \nabla\phi(x) \cdot \nabla\eta(x)\,dx = \int_S m(x)\,\alpha(x)\,\eta(x)\,dx, \tag{2.3}$$

for all test functions $\eta \in \mathcal{H}^1_\alpha(S)$ which vanish at the boundary ∂S. This is because in practice we seek a solution $\phi \in \mathcal{H}^1_\alpha(S)$ with the same property.

A detailed derivation of the existence and uniqueness of a weak solution to PDE (1.1) for a specific choice of coefficients is available in [8]. Since the derivation uses arguments which are standard in the theory of Hilbert spaces, we shall state only the outline.

First, let us consider the following inner-product and norm of the weighted space $\mathcal{H}^1_{\alpha,0}(S)$:

$$\langle v, v' \rangle_{\mathcal{H}^1_{\alpha,0}(S)} \triangleq \int_S \alpha(x) \cdot \nabla v(x) \cdot \nabla v'(x)\,dx, \tag{2.4a}$$

$$\|v\|_{\mathcal{H}^1_{\alpha,0}(S)} = \langle v, v \rangle^{1/2}_{\mathcal{H}^1_{\alpha,0}(S)}, \tag{2.4b}$$

where $v, v' \in \mathcal{H}^1_{\alpha,0}(S)$.

The norm defined in (2.4b) is equivalent to the standard norm in $\mathcal{H}^1_{\alpha,0}(S)$, provided that α satisfies a Poincaré inequality. That is, there exists a constant $C_1 > 0$ (depending only on S and α) such that

$$\int_S (v(x))^2\,\alpha(x)\,dx \leq \frac{1}{C_1}\int_S |\nabla v(x)|^2 \alpha(x)\,dx, \tag{2.5}$$

where $|\cdot|$ denotes the Euclidean norm of a vector. This is in fact the case for coefficients α of the form

$\alpha(x) = \exp(-V(x))$, with $V \in C^2(S)$, $D^2 V \in \mathcal{L}^\infty(S)$, and $|\nabla V(x)| \to \infty$ as $|x| \to \infty$. We describe this particular scenario in § 5.

As a result of (2.5), i) the existence of a solution is assured by the compatibility relation $\int_S m(x)\,\alpha(x)\,dx = 0$ and ii) the uniqueness of a solution is assured by taking a subspace of $\mathcal{H}^1_\alpha(S)$ consisting of functions ϕ for which $\int_S \phi(x)\,\alpha(x)\,dx = 0$, i.e. $\phi \in \mathcal{H}^1_{\alpha,0}(S)$. This leads to the problem of seeking $\phi \in \mathcal{H}^1_{\alpha,0}(S)$ which solves (2.3) for all $\eta \in \mathcal{H}^1_{\alpha,0}(S)$.

In fact, the first step in [8] is to check whether T in the operation $T(\eta) \triangleq \int_S \alpha(x)\cdot\beta(x)\,\nabla\phi(x)\cdot\nabla\eta(x)\,dx$ is a bounded linear operator. If its bound exists, uniqueness of ϕ is shown via the Riesz representation theorem for Hilbert spaces. By limiting ourselves to the subspace $\phi \in \mathcal{H}^1_{\alpha,0}(S)$, the bound is readily shown (see, for instance, Theorem 2.2 in [8]).

2.2 Representing functions by basis functions.

Let $\mathcal{V}^{N_B}$ be a finite-dimensional subspace of $\mathcal{H}^1_{\alpha,0}(S)$ spanned by a collection of N_B basis functions. The idea is to approximate arbitrarily well any $\phi \in \mathcal{H}^1_{\alpha,0}(S)$ by taking a weighted sum of a sufficiently large number N_B of functions $v^{n_B} \in \mathcal{V}^{N_B}$, $n_B = 1, \ldots, N_B$.

Let us introduce the orthogonal projection operator $\mathcal{P}^{N_B} : \mathcal{H}^1_{\alpha,0}(S) \to \mathcal{V}^{N_B}$, i.e. for any $\phi \in \mathcal{H}^1_{\alpha,0}(S)$,

$$\langle \phi - \mathcal{P}^{N_B}\phi, \eta \rangle_{\mathcal{H}^1_{\alpha,0}(S)} = 0, \quad \forall \eta \in \mathcal{V}^{N_B},$$

or equivalently

$$\mathcal{P}^{N_B}\phi(x) = \sum_{n_B=1}^{N_B} \phi^{n_B} v^{n_B}(x),$$

with the arbitrary test function η also written as a weighted sum of functions $v^{n_B} \in \mathcal{V}^{N_B}$.

If $\{\phi^{n_B}\}_{n_B=1}^{N_B}$ and $\{\eta^{n_B}\}_{n_B=1}^{N_B}$ denote the weights for approximating ϕ and η, respectively, we approximate ϕ with $\mathcal{P}^{N_B}\phi(x)$ using weights which obey

(2.6)
$$\sum_{n_B, n'_B=1}^{N_B} \phi^{n_B}\eta^{n'_B} \int_S \alpha(x)\cdot\beta(x)\,\nabla v^{n_B}(x)\cdot\nabla v^{n'_B}(x)\,dx = \sum_{n'_B=1}^{N_B} \eta^{n'_B} \int_S m(x)\,\alpha(x)\,v^{n'_B}(x)\,dx.$$

To simplify (2.6), let us consider an arbitrary index $n^*_B \in \{1, \ldots, N_B\}$, and set $\eta^{n'_B} = \delta(n'_B, n^*_B)$, where δ is the Dirac's delta generalised function. (2.6) becomes

$$\sum_{n_B=1}^{N_B} \phi^{n_B} \int_S \alpha(x)\cdot\beta(x)\,\nabla v^{n_B}(x)\cdot\nabla v^{n^*_B}(x)\,dx = \int_S m(x)\,\alpha(x)\,v^{n^*_B}(x)\,dx.$$

If we let

$$\begin{aligned} u &= (\phi^{n_B})_{n_B=1}^{N_B} \\ A &= \left(\int_S \alpha(x)\cdot\beta(x)\,\nabla v^{n_B}(x)\cdot\nabla v^{n^*_B}(x)\,dx\right)_{n_B,n^*_B=1}^{N_B} \\ b &= \left(\int_S m(x)\,\alpha(x)\,v_{n^*_B}(x)\,dx\right)_{n^*_B=1}^{N_B}, \end{aligned}$$

with $A \in \mathbb{R}^{N_B\times N_B}$ and $b \in \mathbb{R}^{N_B}$, the coefficients $\phi^1, \ldots, \phi^{N_B}$ solve the following linear system

$$Au = b. \tag{2.7}$$

Once we extract these coefficients from u, we get $\mathcal{P}^{N_B}\phi(x) = \sum_{n_B=1}^{N_B} \phi^{n_B} v^{n_B}(x)$.

3 Polynomial basis.

In this section, we construct multivariate polynomial bases. We adopt the orthogonalisation method from [9] to generate orthogonal bases suitable for potentially correlated variables, that is, the case where the coefficient α is not necessarily factorisable.

The series of N_X-dimensional functions $\{v^{n_B}(x)\}_{n_B=1}^{N_B}$ is possibly orthogonal with respect to α. For each $n_B, n'_B = 1, \ldots, N_B$,

$$\langle v^{n_B}, v^{n'_B}\rangle_{\mathcal{H}^1_{\alpha,0}(S)} = \|v^{n_B}\|^2_{\mathcal{H}^1_{\alpha,0}(S)}\delta_{n_B n'_B}.$$

When α is factorisable as $\alpha(x) = \prod_{n_X=1}^{N_X} \alpha_{n_X}(x_{n_X})$, each v^{n_B} is a tensor product of one-dimensional functions, i.e. $v^{n_B}(x) = \prod_{n_X=1}^{N_X} v^{n_B}_{n_X}(x_{n_X})$. In the general case, the bases are mutually orthogonal with respect to α using orthogonalisation methods.

The method from [9] projects an arbitrary basis onto a subspace with a suitable inner product. The first step is the initial choice of basis, e.g. a set of linearly independent polynomials. Any such set can be used, but for simplicity, we consider $\{e^{n_B}(x)\}_{n_B=1}^{N_B}$ given by

$$e^{n_B}(x) = P^{k^{n_B}}(x) \triangleq \prod_{n_X=1}^{N_X} \frac{(x_{n_X} - \mu_{n_X})^{k^{n_B}_{n_X}}}{k^{n_B}_{n_X}!}, \tag{3.8}$$

where $k^{n_B} = (k^{n_B}_1, \ldots, k^{n_B}_{n_X}, \ldots, k^{n_B}_{N_X})$ is a collection of exponents with $k^{n_B}_{n_X} \in \{0, \ldots, K\}$, K is a discretisation parameter, while P denotes polynomial and $\mu = (\mu_1, \ldots, \mu_{n_X}, \ldots, \mu_{N_X})$ is a collection of shift parameters.

The discretisation parameter K represents the highest univariate polynomial degree. For a fixed dimension N_X, it determines the number N_B of functions used to approximate ϕ. For example, for $N_X = 2$, $K = 2$, and $\mu = (0, 0)$, we obtain the following set of functions for a variable $x = (x_1, x_2)$:

$$\left\{1, x_1, x_2, x_1x_2, \frac{x_1^2}{2}, \frac{x_2^2}{2}, \frac{x_1^2 x_2}{2}, \frac{x_1 x_2^2}{2}, \frac{x_1^2 x_2^2}{4}\right\},$$

and thus $N_B = 9$.

If the collection $\{v^{n_B}(x)\}_{n_B=1}^{N_B}$ is not orthogonal, the resulting matrix A in (2.7) may be dense, making the linear system generally more costly to solve. An orthogonal $\{v^{n_B}(x)\}_{n_B=1}^{N_B}$ is constructed from $\{e^{n_B}(x)\}_{n_B=1}^{N_B}$ using the Gram-Schmidt process

$$v^1(x) = e^1(x)$$

$$v^{n_B}(x) = e^{n_B}(x) - \sum_{n'_B=1}^{n_B-1} c_{n_B n'_B} v^{n'_B}(x) \text{ for } 2 \le n_B \le N_B,$$

where the coefficients $\{c_{n_B n'_B}\}_{2 \le n_B \le N_B, 1 \le n'_B < N_B}$ are

$$c_{n_B n'_B} = \frac{\langle e^{n_B}, v^{n'_B}\rangle_{\mathcal{H}^1_{\alpha,0}(S)}}{\langle v^{n'_B}, v^{n'_B}\rangle_{\mathcal{H}^1_{\alpha,0}(S)}},$$

with the inner-product defined in (2.4a).

Smoothing estimates with a roughness penalty. The roughness of the estimate for ϕ can be controlled by the number N_B of basis functions. If the derivative of order r is the highest required, one can also control the curvature of the highest order derivative by penalising the derivatives of order $r + 2$ [10, Chapter 5].

Let $D^r = \left(D^r_{x_1}, \ldots, D^r_{x_{N_X}}\right)$ denote the r-th order differentiation where $D^r_{x_{n_X}}$ is differentiation with respect to the n_X-th coordinate of x. Using the penalty

$$\text{PEN}_r(\phi) = \|D^r \phi\|^2_{\mathcal{L}^2_\alpha(S)} \tag{3.9}$$

implies that the heavier the penalty, the more ϕ will approximate a polynomial of order $r - 1$ weighted by $\alpha^{1/2}$. The penalised estimate often does much better at the boundaries of ϕ than the non-penalised one.

The penalty (3.9) applied to the space $\mathcal{V}^{N_B}$ can be expressed in matrix terms as $\text{PEN}_r(\phi) = \phi^\top R \phi$, where ϕ is a concatenation of $\{\phi^{n_B}\}_{n_B=1}^{N_B}$, and the positive semi-definite matrix R contains elements

$$R_{n_B n'_B} = \langle D^r v^{n_B}, D^r v^{n'_B}\rangle_{\mathcal{L}^2_\alpha(S)},$$

with $v^{n_B}, v^{n'_B} \in \mathcal{V}^{N_B}$, and $n_B, n'_B = 1, \ldots, N_B$.

Adding a roughness penalty to the linear system (2.7) is equivalent to finding u according to

$$(A + \zeta R)\, u = b, \quad \zeta \ge 0. \tag{3.10}$$

Although any non-negative value of ζ can be considered, floating-point computation limits the implementation of (3.10). The matrices A and R can differ in size, and with $\text{rank}(R) \le N_B - r$, R cannot be treated as a coefficient matrix. Thus, ζR must not overwhelm A.

One technique for choosing ζ is the generalised cross-validation (GCV) method developed in [11]. Let $\hat{b}$ denote the reconstructed fit of b using a roughness penalty. Then the GCV criterion is expressed as

$$\text{GCV}(\zeta) = \frac{1}{N_B - df(\zeta)} \cdot \frac{|b - \hat{b}|^2}{N_B - df(\zeta)}, \tag{3.11}$$

where $df(\zeta)$ is the effective degree of freedom. Notably, (3.11) allows for the selection of ζ that minimises the error of the fit while accounting for model complexities.

In the case of (3.10), the criterion (3.11) becomes

$$\text{GCV}(\zeta) = \frac{|\left(I_{N_B \times N_B} - G(\zeta)\right) b|^2}{\left(N_B - \text{tr}\left(G(\zeta)\right)\right)^2}, \tag{3.12}$$

where $G(\zeta)$ is a matrix used to reconstruct b via $\hat{b} = G(\zeta)\, b$, and it takes the form

$$G(\zeta) \triangleq A\left(A^\top A + \zeta R\right)^{-1} A^\top,$$

with corresponding effective degree of freedom $df(\zeta) = \text{tr}(G(\zeta))$.

Having addressed the choice of basis functions and the use of regularisation, we now proceed to incorporate sparsity into the approximations. The goal is to improve approximation accuracy by increasing the number of basis functions, while ensuring computational feasibility for moderate-dimensional problems.

4 Hyperbolic cross approximation.

In addition to the notation introduced in Table 1, we define the following section-specific terms:

- $k = (k_1, \ldots, k_{n_X}, \ldots, k_{N_X})$ is a multi-index vector, where $k_{n_X} \in \mathbb{N}_0$ for all $n_X = 1, \ldots, N_X$. That is, $k \in \mathbb{N}_0^{N_X}$.
- The frequently used norms in $\mathbb{N}_0^{N_X}$ are denoted as

$$|k|_1 = \sum_{n_X=1}^{N_X} k_{n_X}, \quad |k|_\infty = \max_{1 \le n_X \le N_X} k_{n_X},$$

$$|k|_{\text{mix}} = \prod_{n_X=1}^{N_X} \max\{1, k_{n_X}\}.$$

Besides the discretisation parameter $K \in \mathbb{N}$, we consider a sparsity level $\epsilon \in (-\infty, 1]$ to define generalised sparse grid spaces as in [6]:

$$\mathcal{I}_{K,\epsilon} = \left\{ k \in \mathbb{N}_0^{N_X} : |k|_{\text{mix}} |k|_\infty^{-\epsilon} \leq K^{1-\epsilon} \right\}.$$

The parameter ϵ stems from optimising the cost and accuracy of the sparse space with respect to an energy seminorm [12]. Based on the index set $\mathcal{I}_{K,\epsilon}$, the corresponding finite-dimensional subspace is

$$\mathcal{V}^{N_B} = \text{span}\left\{ P^k : k \in \mathcal{I}_{K,\epsilon} \right\},$$

and the collection $\{v^{n_B}(x)\}_{n_B=1}^{N_B}$ is then constructed from orthogonalisation of (3.8) with $k \in \mathcal{I}_{K,\epsilon}$.

The set $\{P^k\}_{k \in \mathcal{I}_{K,\epsilon}}$ is dense in $\mathcal{H}^1_{\alpha,0}(S)$, meaning that any function in this space can be approximated arbitrarily well as $K \to \infty$. This follows from results on polynomial approximation in weighted Sobolev spaces. A sufficient condition is that α is continuous and finite in S, and has an exponential decay [13].

The relationship between the cardinality N_B and the parameter K is now conditional on ϵ. In practice, ϵ allows us to switch from the full grid case $\epsilon \to -\infty$ to the hyperbolic cross case $\epsilon = 0$. It also allows us create with $\epsilon \in (0, 1]$ subspaces of the hyperbolic cross space with further reduced complexities, as shown in Figure 1.

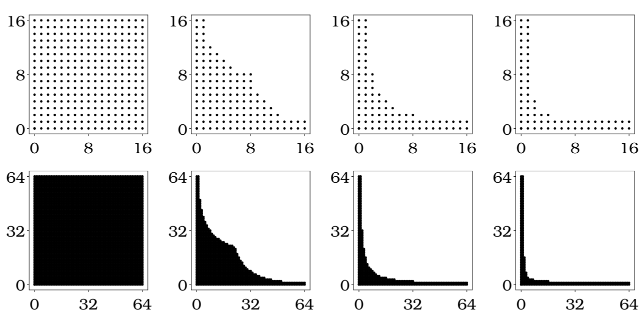

Figure 1: Index sets $\mathcal{I}_{16,\epsilon}$ (top) and $\mathcal{I}_{64,\epsilon}$ (bottom) for $\epsilon \to -\infty$ and $\epsilon = -2, 0, 0.5$ (from left to right), $N_X = 2$.

The complexities are as follows:

- $\epsilon \to -\infty$ corresponds to the N_X-dimensional full tensor grid, indexed by the set

  $$\mathcal{I}_{K,-\infty} = \left\{ k \in \mathbb{N}_0^{N_X} : |k|_\infty \leq K \right\},$$

  with corresponding finite-dimensional subspace

  $$\mathcal{V}^{N_B} = \text{span}\left\{ P^k : k \in \mathcal{I}_{K,-\infty} \right\},$$

  and cardinality N_B (number of indexed basis functions) known to depend exponentially on the dimension of the state space, $N_B = (K+1)^{N_X}$.
- $\epsilon = 0$ corresponds to the so-called regular hyperbolic cross approximation. N_B is $\mathcal{O}(K(\ln K)^{N_X - 1})$.
- $0 < \epsilon \leq 1$ corresponds to the so-called optimal hyperbolic cross approximation. The curse of dimensionality with respect to N_X, which still was present when $\epsilon = 0$, has now disappeared: N_B is $\mathcal{O}(K)$. The question is if for $\epsilon \in (0, 1]$, the accuracy deteriorates exponentially with N_X or is maintained. We investigate this in a future publication.

5 Particle Flow.

In this section, we explore an instance of PDE (1.1) where α is the density of particles drawn from a probability distribution, and whose transport is affected by an external force m linked to the likelihood of the particles with respect to observations. This is one of the core problems in particle flow for solving Bayesian statistical problems. Its successful treatment would allow sampling from complex distributions without facing particle degeneracy and sample impoverishment.

Let us denote by π_0 the prior probability distribution of an N_X-dimensional random variable X, and by π_1 the probability distribution of X conditional on y, a given observation. The probability density function of π_1, denoted p_1, is computed using Bayes' rule as follows:

$$p_1(x) = \frac{p_0(x)\, p(y|x)}{z}, \tag{5.13}$$

where $p(y|x)$ represents the likelihood of observing y given x, p_0 is the probability density function of π_0, and z is a normalising factor.

To briefly introduce particle flow, we start by letting *i)* $C_X = C_X([0,1], \mathbb{S}_X)$ be the space of continuous functions on the time index set $[0,1]$ that take values in $\mathbb{S}_X \subseteq \mathbb{R}^{N_X}$, and *ii)* $\mathbb{S}_Y$ be a complete separable metric space such that regular conditional probabilities exist.

We introduce a pseudo-time variable λ in $[0,1]$, which parametrises a density function $p(\lambda, \cdot)$ satisfying

$$p(\lambda, x) = \frac{p_0(x) p^\lambda(y|x)}{z(\lambda)},\ x \in S,\ S \subseteq \mathbb{S}_X, \tag{5.14}$$

where the normalising factor $z(\lambda)$ is such that $p(\lambda, x)$ remains a probability density function for all $\lambda \in [0,1]$. Equations (5.13) and (5.14) are linked by setting

$$p(0, x) = p_0(x), \quad p(1, x) = p_1(x),$$

that is, $p(0,x)$ is the probability density function of the prior and $p(1,x)$ is that of the posterior.

In particle flow, we seek a (possibly random) process $X = (X_\lambda, \lambda \in [0,1])$ for which the probability density function of X_λ is exactly $p(\lambda, \cdot)$ for all $\lambda \in [0,1]$. If such process exists, π_0 is given, $X_0 \sim \pi_0$ and $X_1 \sim \pi_1$, we then call X a particle flow.

Let us assume that X has the following evolution:

$$dX_\lambda = f_\lambda(X)\, d\lambda, \quad X_0 = x_0, \tag{5.15}$$

where x_0 is distributed according to π_0.

In (5.15), $f_\lambda : C_X \to \mathbb{R}^{N_X}$ is chosen such that the distribution of X_λ has density $p(\lambda, \cdot)$. Different choices of the functional f_λ lead to different flows X. In this work, we let $(\Omega, \mathcal{F}, \mathbb{P})$ be the appropriate probability space for our processes, and restrict ourselves to functionals f_λ that depend only on $X(\omega)$ at pseudo-time λ, where $X(\omega)$ is the sample path, or trajectory, of X associated with $\omega \in \Omega$. That is, $f_\lambda(X) = f_\lambda(X_\lambda)$, implying that X is a Markov process. Given p_0 on $\mathbb{S}_X$, p satisfies the continuity equation

$$\frac{\partial}{\partial \lambda} p(\lambda, x) = -\sum_{n_X=1}^{N_X} \frac{\partial}{\partial x_{n_X}} [f_\lambda^{n_X}(x)\, p(\lambda, x)], \tag{5.16}$$

with initial condition $p(0, x) = p_0(x)$.

Furthermore, the flow is assumed to be of gradient type, meaning that for any $\lambda \in [0,1]$, f_λ minimises

$$J_\lambda(g) = \frac{1}{2} \int_S g^\top g(x)\, p(\lambda, x)\, dx$$

over all admissible vector fields $g : \mathbb{S}_X \to \mathbb{R}^{N_X}$.

This happens when f_λ takes the form $f_\lambda(x) = M^{-1}(\lambda, x) \nabla_x \phi(\lambda, x)$, where $\phi : [0,1] \times \mathbb{S}_X \to \mathbb{R}$ represents a dynamic potential function, ∇_x is the gradient operator with respect to x, and M is a symmetric positive semi-definite matrix acting as a preconditioner. Therefore, letting $\nabla_x \cdot (\cdot)$ denote the divergence operator with respect to x, (5.16) can be rewritten as

$$\frac{\partial}{\partial \lambda} p(\lambda, x) = -\nabla_x \cdot \left(p(\lambda, x) \cdot M^{-1}(\lambda, x) \nabla_x \phi(\lambda, x) \right). \tag{5.17}$$

We may write $p(y|x)$ in (5.13) in terms of the negative log-likelihood $L(x, y)$, that is, $p(y|x) = \exp(-L(x, y))$. Then the following identity must hold:

$$\frac{\partial}{\partial \lambda} p(\lambda, x) = -(L(x, y) - \overline{L}(\lambda, y)) p(\lambda, x), \tag{5.18}$$

where $L : \mathbb{S}_X \times \mathbb{S}_Y \to \mathbb{R}$ and $\overline{L} : [0,1] \times \mathbb{S}_Y \to \mathbb{R}$, with

$$L(x, y) \triangleq -\log p(y|x), \; \overline{L}(\lambda, y) \triangleq \int_S L(x, y)\, p(\lambda, x)\, dx.$$

By comparing the right-hand sides of (5.17) and (5.18), we obtain the following PDE of interest:

$$\begin{aligned} -\nabla_x \cdot \left(p(\lambda, x) \cdot M^{-1}(\lambda, x) \nabla_x \phi(\lambda, x) \right) \\ = -(L(x, y) - \overline{L}(\lambda, y)) p(\lambda, x). \end{aligned} \tag{5.19}$$

Notably, this PDE is a special case of PDE (1.1),

$$\begin{aligned} -\nabla \cdot (\alpha(x) \cdot \beta(x) \nabla \phi(x)) = m(x)\, \alpha(x), \\ \int_S m(x)\, \alpha(x)\, dx = 0, \; x \in S, \; S \subseteq \mathbb{S}_X, \end{aligned}$$

where $\alpha(x) = p(\lambda, x)$, $\beta(x) = M^{-1}(\lambda, x)$, $\phi(x) = \phi(\lambda, x)$, and $m(x) = -(L(x, y) - \overline{L}(\lambda, y))$, for fixed values of pseudo-time λ and observation y.

5.1 Numerical experiments. In this section, we present the results obtained by combining the spectral representation (§3) of the solution to PDE (5.19) with the hyperbolic cross approximation (§4), when applied to Gaussian and non-Gaussian posterior distributions.

Here, the probability density functions take the form $p(\lambda, x) = \exp(-V(x))$, for all $\lambda \in [0,1]$. Moreover, V satisfies the conditions outlined in 2.1 for existence of a unique solution to the corresponding PDE.

To evaluate our results, we use the Kullback–Leibler (KL) divergence as a comparative metric between two probability distributions. Given two probability densities, q and p, defined on $S \subseteq \mathbb{S}_X$, the KL divergence of q relative to p is given by

$$\mathrm{KL}(q, p) = \int_S \log \frac{q(x)}{p(x)} q(x)\, dx. \tag{5.20}$$

This quantity is always non-negative and equals zero if and only if q and p are identical almost everywhere. Lower values indicate that q is closer to p, while higher values imply greater divergence.

We work with the following Monte Carlo-based estimator of the integral in (5.20):

$$\widehat{\mathrm{KL}}(q, p) = \frac{1}{N_P} \sum_{n_P=1}^{N_P} \left(r\left(X^{(n_P)}\right) - \log r\left(X^{(n_P)}\right) + 1 \right), \tag{5.21}$$

where $r(x) = \frac{p(x)}{q(x)}$, and $\left\{X^{(n_P)}\right\}_{n_P=1}^{N_P}$ are samples drawn from a probability distribution with density function q.

Hereafter, p denotes the reference density, while q is approximated by a kernel density estimator $\hat{q}$:

$$\hat{q}(x) = \frac{1}{N_P l_1 \cdots l_{N_X}} \sum_{n_P=1}^{N_P} \left\{ \prod_{n_X=1}^{N_X} \kappa\left(x^{n_X}, X^{(n_P)n_X}; l_{n_X}\right) \right\},$$

where $\{l_{n_X}\}_{n_X=1}^{N_X}$ are scaling parameters of a suitable kernel κ. For simplicity, we set the kernel $\kappa(a, a'; l)$ to be the squared-exponential kernel $\kappa(a, a'; l) = \exp\left(-\left(\frac{a-a'}{l}\right)^2\right)$. The scaling parameters are selected according to the leave-one-out likelihood criterion [14].

To assess our proposed spectral method equipped with the hyperbolic crossing approximation (GHC), we compare its resulting approximation of the posterior distribution with the results from two other techniques. Specifically, we will contrast GHC with the diffusion-map technique (KERNEL), also often used in particle flow [1, 4], and with the importance sampling technique (IS), standard in the Monte Carlo literature.

For GHC and KERNEL, we need to solve (5.15) by integrating it from $\lambda = 0$ to $\lambda = 1$. However, we must first obtain $f_\lambda(x) = M^{-1}(\lambda, x)\nabla_x\phi(\lambda, x)$, $\lambda \in [0,1]$. For this, we let $M^{-1}(\lambda, x) = I_{N_X \times N_X}$ and ϕ be the approximated solution to (5.19), either by our proposed spectral method or by diffusion-maps.

There are several parameter choices in GHC and KERNEL that will affect the performance. For GHC, the maximum order K, the sparsity level ϵ, and the smoothing parameters r and ζ are the main parameters to tweak. For KERNEL, its length-scale parameter is the most important. As in [15], we have not spent much effort in tuning these to each particular example, and it is likely that better performance can be achieved by adjusting the values of these parameters. However, ζ in GHC was set to be the minimiser of the generalised cross-validation criteria in (3.12), and the length-scale parameter in KERNEL follows the median criterion for bandwidth selection from [16], as suggested in [1].

5.1.1 Gaussian distribution.

Let us consider the Bayes' rule when the prior and posterior distributions are given by, respectively, $\pi_0 = \mathcal{N}((0,\ldots,0), I_{N_X\times N_X})$, and $\pi_1 = \mathcal{N}((1,\ldots,1), I_{N_X\times N_X})$. To transition from π_0 to π_1, we set $p(y|x) \propto \exp\left(\sum_{n_X=1}^{N_X} x\right)$.

This example is chosen because, as N_X increases, the two measures become exponentially singular with respect to each other. Consequently, the particle flow technique is expected to outperform traditional Bayesian computational methods, such as IS.

We compute the estimator $\widehat{\mathrm{KL}}$ for the KL divergence between π_1 and the empirical posterior distribution from an ensemble of $N_P = 256$ particles. To demonstrate the challenge of approximating the posterior as N_X grows, we consider $N_X \in 2,4,6,8$ and report the mean $\widehat{\mathrm{KL}}$ over 20 runs per dimension. Results are shown in Table 2.

Table 2: $\widehat{\mathrm{KL}}$ for Gaussian posterior distribution.

N_X	IS	KERNEL	GHC
2	1.96	0.31	**0.15**
4	9.57	3.04	**1.09**
6	18.16	13.68	**3.19**
8	26.09	30.65	**6.49**

As expected, the KL divergence for IS rises significantly, indicating a poor approximation due to the increasing singularity between the prior and posterior. KERNEL performs well in lower dimensions but diverges for larger N_X for this choice of N_P. Conversely, GHC maintains relatively lower $\widehat{\mathrm{KL}}$ values across dimensions. This result aligns with expectations, as spectral methods are the standard reference in the particle flow literature for Gaussian distributions.

5.1.2 Rosenbrock distribution.

The second example is a two-dimensional benchmark model from [17]: the Rosenbrock distribution. We chose this distribution for its desirable properties in Monte Carlo testing, such as a complex density structure, an easy extension to arbitrary dimensions, and a known normalising factor.

In this example, the Rosenbrock distribution has a conditionally Gaussian component. Specifically, for $X = (X^{(1)}, X^{(2)})$, if $X^{(1)} \sim \mathcal{N}(\mu, \sigma)$, then $X^{(2)}|X^{(1)} \sim \mathcal{N}((X^{(1)})^2, \sigma)$. In this case, we set $\mu = 0$ for the prior distribution and $\mu = 1$ for the posterior distribution, with a standard deviation of $\sigma = 0.5$.

Table 3: $\widehat{\mathrm{KL}}$ for Rosenbrock posterior distribution.

Method	$N_P = 256$	$N_P = 512$
IS	1.39	1.36
GHC ($\epsilon \to -\infty$)	0.68	0.32
GHC ($\epsilon = -2$)	**0.24**	**0.17**
GHC ($\epsilon = 0$)	0.29	**0.17**
GHC ($\epsilon = 0.5$)	0.31	0.18
KERNEL	0.43	0.35

Table 3 presents the estimated KL divergence between π_1 and the empirical posterior distribution for different methods. As expected, increasing the number of particles from $N_P = 256$ to $N_P = 512$ generally reduces KL divergence values, indicating a better approximation. The decrease in KL divergence for $\epsilon = -2$ and $\epsilon = 0$ is likely due to fewer basis coefficients being approximated. Although incorporating more functions generally leads to better approximations, this is not necessarily the case for (3.10) implemented using Monte Carlo estimates with a finite N_P: the estimates for A, R and b based on higher-order polynomials can exhibit significant variability. Conversely, for the case of subspaces of the hyperbolic cross space, $\epsilon \in (0, 1]$, we expect the approximation to deteriorate as ϵ increases, as higher sparsity may result in losing important basis functions that capture correlations across dimensions. However, the resulting values in Table 3 remain reasonable, indicating that even for $\epsilon > 0$, the method still provides a good approximation.

To conclude this section, we illustrate one of the experiments used for Tables 2 and 3. Figure 2 displays the estimated posterior density functions.

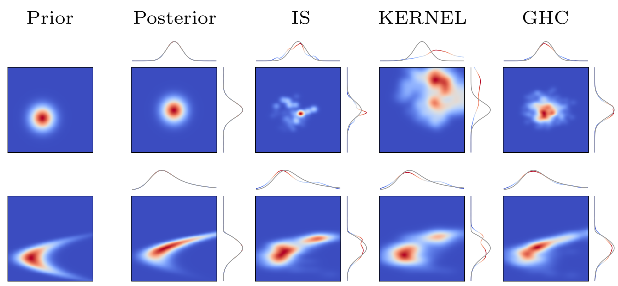

Figure 2: 8-dimensional Gaussian prior and posterior density functions (top) and two-dimensional Rosenbrock prior and posterior density functions (bottom). Marginal density functions are represented by marginal curves. Red regions indicate areas of higher probability mass. For the Gaussian case, only the first two coordinates are shown. Kernel density estimators are based on $N_P = 256$ particles using IS, KERNEL, and GHC.

6 Concluding remarks.

In this work, we proposed a spectral method to solve the weighted Poisson equation (1.1). Within the context of sequential Monte Carlo, we examined our choice of basis and the approximation to the solution when adjusting the sparsity level of the tensor product.

In an extended version of this work, we intend to *i*) establish error bounds for GHC-based approximations in $\mathcal{H}^1_{\alpha,0}(S)$, and *ii*) apply GHC-based particle flow to state-estimation problems, in which the posterior distribution is conditional on a given stream of observations y. To better understand the accuracy deterioration with N_X for $\epsilon \in (0, 1]$, we also intend to solve the weighted Poisson equation associated with a fixed value of λ, using quadrature rules in place of the Monte Carlo integration, while omitting the regularisation term. This setting would isolate the effect of the choice of basis and the associated sparsity from the noise introduced by sampling and regularisation.

Acknowledgments.

Muhammad Emzir would like to acknowledge the support he received from DROC KFUPM (grant no. ER242009) and IRC smart mobility and logistics (grants no. INML2528 and no. INML2407).

References

[1] Amirhossein Taghvaei, Prashant G. Mehta, and Sean P. Meyn. Diffusion map-based algorithm for gain function approximation in the feedback particle filter. *SIAM/ASA Journal on Uncertainty Quantification*, 8(3):1090–1117, 2020.

[2] Karl Berntorp and Piyush Grover. Data-driven gain computation in the feedback particle filter. In *American Control Conference*, 2016.

[3] Tao Yang, Richard S. Laugesen, Prashant G. Mehta, and Sean P. Meyn. Multivariable feedback particle filter. *Automatica*, 71:10–23, 2016.

[4] Amirhossein Taghvaei and Prashant G. Mehta. A survey of feedback particle filter and related controlled interacting particle systems (CIPS). *Annual Reviews in Control*, 55:356–378, 2023.

[5] C. Canuto, M. Y. Hussaini, A. Quarteroni, and T. A. Zang. *Spectral Methods: Fundamentals in Single Domains*. Scientific Computation. Springer, 2007.

[6] Michael Griebel and Jan Hamaekers. Sparse grids for the Schrödinger equation. *Modélisation mathématique et analyse numérique*, 41(2):215–247, 2007.

[7] Xue Luo and Stephen S.-T. Yau. Hermite spectral method with hyperbolic cross approximations to high-dimensional parabolic pdes. *SIAM Journal on Numerical Analysis*, 51(6):3186–3212, 2013.

[8] Richard S. Laugesen, Prashant G. Mehta, Sean P. Meyn, and Maxim Raginsky. Poisson's equation in nonlinear filtering. *SIAM Journal on Control and Optimization*, 53(1):501–525, 2015.

[9] John D. Jakeman, Fabian Franzelin, Akil Narayan, Michael Eldred, and Dirk Pflüger. Polynomial chaos expansions for dependent random variables. *Computer Methods in Applied Mechanics and Engineering*, 351:643–666, 2019.

[10] J. Ramsay and B. W. Silverman. *Functional Data Analysis*. Springer Series in Statistics. Springer, 2005.

[11] Grace Wahba and Peter Craven. Smoothing noisy data with spline functions. *Numerische Mathematik*, 31:377–404, 1979.

[12] Hans-Joachim Bungartz and Michael Griebel. A note on the complexity of solving poisson's equation for spaces of bounded mixed derivatives. *Journal of Complexity*, 15(2):167–199, 1999.

[13] José M. Rodríguez. Approximation by polynomials and smooth functions in sobolev spaces with respect to measures. *Journal of Approximation Theory*, 120(2):185–216, 2003.

[14] Adrian W. Bowman. An alternative method of cross-validation for the smoothing of density estimates. *Biometrika*, 71(2):353–360, 1984.

[15] Karl Berntorp. Comparison of gain function approximation methods in the feedback particle filter. In *21st International Conference on Information Fusion (FUSION)*, pages 123–130, 2018.

[16] Arin Chaudhuri, Deovrat Kakde, Carol Sadek, Laura Gonzalez, and Seunghyun Kong. The mean and median criteria for kernel bandwidth selection for support vector data description. In *IEEE International Conference on Data Mining Workshops*, pages 842–849, 2017.

[17] Filippo Pagani, Martin Wiegand, and Saralees Nadarajah. An n-dimensional Rosenbrock distribution for Markov chain Monte Carlo testing. *Scandinavian Journal of Statistics*, 49(2):657–680, 2022.